Premier Journal of Engineering and Applied Sciences
Publication of Nigerian Society of Engineers, Ibadan Branch
P J E A S
Vol. 5, No. 2, 2024 ISSN:2734-3170

Analytical Study and Modelling of a Multi-Finger Robotic Hand

A. Adus and T. S. Amosun*

Department of Mechanical and Mechatronic Engineering, Federal University of Otuoke, Bayelsa, Nigeria

***Corresponding Author:** *amosunts@fuotuoke.edu.ng*

ARTICLE INFO

Received: February, 2024
Accepted: April, 2024
Published: April, 2024

Keywords:
Analytical
Electromechanical
Kinematic
Modelling
Robot.

ABSTRACT

The desire to reduce or eliminate human labour led to the development of robots. Essentially, a robot is an electromechanical device controlled by computers and electronic programming. It can be remotely controlled, autonomous or semi-autonomous. The analysis of trajectory generation of arm and finger robots is carried out in this work by using kinematic formulations based on coordinate transformation matrices obtained from the Denavit-Hartenberg convention. This involves the methodical process of deriving equations using homogeneous transformations. The joint torque is also determined by dynamic analysis using the moment principle method. To move the joints and limbs in the robot hand, joint torque is required. After completing the torque calculation, the optimal proportional-integral-derivative controller design was achieved without affecting the development of the general transfer function and mathematical model. Simulation was used to determine whether or not the analysis was suitable for system control.

1. INTRODUCTION

Kinematics studies motion without considering the forces that cause it and also examines position, acceleration, velocity as well as all higher order derivatives of the position variable. This also includes examining geometric and time-based motion properties, as well as changes in the way the different limbs move relative to each other and over time. According to Hu *et al.* (2023), it facilitates the derivation of dynamic properties that must be considered for servo control and thus for movement. Robotic hands carried out several astonishing functions similar to the human hands, hence offering high flexibility in terms of the tasks performed (Kim *et al.*, 2021). The numerous robotics studies conducted over the years have shown that to develop a functional multi-fingered robotic hand, researchers need a thorough understanding of some key parameters related to the movement of the robot manipulator.

Liu and Zhang (2024) presented a novel metamorphic multi-fingered robotic hand. This study detailed the structure of the metamorphic hand that comprised an articulated palm and fingers. It went further to analyze the design parameters of the metamorphic hand's hybrid structure and proposed analytical models for both forward and inverse kinematics. Woi *et al.* (2020) used AUBO-15 manipulator for kinematic analysis and trajectory planning. The study established the AUB-15 manipulator by M-D-H method and the homogeneous transformation matrix between corresponding coordinate was calculated. Furthermore, Neha *et al.* (2021) discussed the grasp capability analysis of the four-finger tendon-actuated robotic hand and also developed the mathematical model for cylindrical shaped objects. An artificial hand with hierarchical reflex control similar to that of a human was created by Folgheraite and Gini (2001). Massa *et al.* (2002) developed an under-powered prosthetic hand.

For multi-finger manipulation, Krausz and Rorrer (2015) designed and fabricated a six degree-of-freedom open source hand. A design and motion analysis of a bio-inspired soft robotic finger based on multi-sectional soft reinforced actuator was also proposed by Janghorban and Dehghani (2022). Mina *et al.* (2008) discovered the joint of the robot finger using inverse kinematics. A humanoid robot hand was modeled by Yunus and Hacioghi (2009) in the dynamic model aspect. Majidi *et al.* (2021) presented a comprehensive review of soft and rigid wearable rehabilitation and assistive devices with a focus on the shoulder joint. Aguilar and Castillo (2016) designed a reconfigurable robotic system for flexo-extension fitted to hand fingers size. Equations for kinematics and dynamics were derived by Psarasuraman (2008) for the purpose of biomechanical analysis of human joints. Kinematic and dynamic designs are not separate problems; kinematic properties may need to be modified to determine acceptable values for a robot's dynamic properties. Therefore, it is ideal if the dynamic and kinematic properties are present at the same time. This study carried out the kinematic analyses of three-finger robot hand development.

2. METHODOLOGY

The multi-finger robot hand has ten degrees of freedom. The hand consists of three fingers and four limbs: the fixed base limb and three movable limbs. The robot hand can move its fingers individually but cannot control each joint segment individually. The hand consists of three servo motors; each is attached to the base connection, allowing flexion at each joint. The lack of independent movement at each joint requires the creation of a transmission mechanism. The only goal of a linkage-based mechanism is to transmit the torque generated by the servomotor from the base to the fourth phalanx or distal phalanges. The connecting link connects each finger segment, giving the hand a realistic imitation of the grasping movements of a human hand.

The individual joint values for each finger joint are the collective variables that need to be mapped for the purposes of this study. These values form the joint space of the multi-fingered robot hand. Joint values (joints θ_i, i = 1, 2 and 3) result in a total of three joint values. A value that corresponds to the user's particular understanding is created by combining these values into one. System design requires the use of unconventional methods to replicate human characteristics such as soft tissue, compliant behavior and structure. Defining the kinematic structure of the hand and its fingers, creating new actuators with precise torque/velocity capabilities and dimensions, and integrating novel sensor types (position, force, torque, and tactile sense) into the hand all play an important role in further development skilled robot hands. A synthesis procedure based on the analyzed features yielded the proposed finger mechanism, which is presented. Using SolidWorks 2012, motion analysis and Finite Element Analysis (FEA) were used to test the proposed design solution.

2.1 Forward Kinematics Analysis

Regarding the robot joint variables, forward kinematics is used to determine the position and orientation of the three-finger robot hand with respect to the robot base coordinate system. If a robot joint is prismatic, its variables are joint extension; in a swivel joint, these are the angles between the links. The joints in this study are all rounded. By repeatedly multiplying the homogeneous transformation matrices H between successive connections as given in equation 1, one can obtain the transformation matrix used to determine the orientation and position of the three-fingered robot hand in the base coordinates. The steps taken to create the forward kinematics equation are discussed.

$$H_0^4 = [H_0^1 H_1^2 H_2^3 H_3^4] \quad (1)$$

Where H_0^1, H_1^2, H_2^3 and H_3^4 are the homogeneous transformation matrices between the links.
H_0^4 = Orientation and position of the three-fingered robot hand in the base coordinates.
Subscripts 0,1,2,3 and 4 are representing base link and links 1, 2 and 3 respectively.
Superscripts 1, 2, 3 and 4 are also representing links 1, 2, 3 and 4 respectively.

Premier Journal of Engineering and Applied Sciences
Publication of Nigerian Society of Engineers, Ibadan Branch
P J E A S
Vol. 5, No. 2, 2024 ISSN:2734-3170

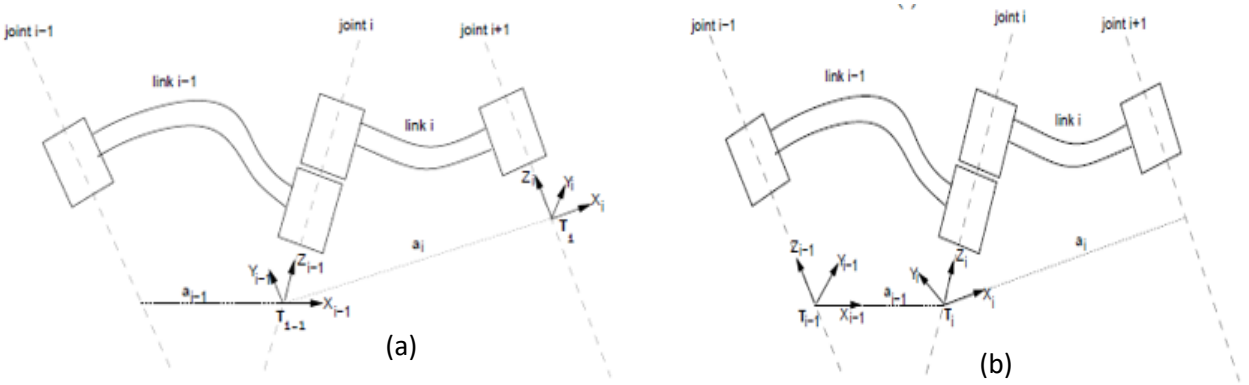

Figure 1: (a) Standard form and (b) modified form of a three-link planar model (single finger)

I. Obtain the Devanit-Hartenberg (DH) Parameters

The DH Parameters namely link length, link twist, link offset and joint angle are necessary to derive the forward kinematic equation for the three-fingered robot hand. These parameters are listed in Table 1 below.

Table 1: Finger parameters using Devanit-Hartenberg convention

Link	Joint (j)	$Joint\ angle$ $\theta i\ (degree)$	Link offset $d_i\ (mm)$	$Link\ length$ $ai\ (mm)$	Link twist $\alpha i\ (degree)$
1	0-1	θ_1	0	0	0
2	1-2	θ_2	0	50	0
3	2-3	θ_3	0	45	0
4	3-4	0	0	35	0

II. Obtain the link transformation matrix A_i (A Matrices)

It is possible to derive several homogeneous matrices based on the number of Degree of Freedom (DOF) after obtaining the DH convention table. One can compute the transformation matrix for every joint ranging from joint 1 to joint i using equation 2.

$$A_i = Rot(z, \theta_i)Trans(z, d_i)Trans(x, a_i)Rot(x, \alpha_i) \quad (2)$$

Where z_i: axis of actuation for joint i+1

θ_i: the angle between x_{i-1} and x_i measured about z_{i-1} . θ_i is variable if joint i is revolute.

d_i: distance along z_{i-1} from 0_{i-1} to the intersection of the x_i and z_{i-1} axes. d_i is variable if joint i is prismatic.

x_i: axis of actuation for joint i+1.

III. Obtain the manipulator transformation matrix H_i^0 MATRIX.

A simple method to determine the total homogeneous matrix for the *4-links* 3-finger robot manipulator is to multiply all the transformation matrices from $T_0^1\ to\ T_3^4$ as in equation 3. This is done after the homogenous matrix has been defined for each link of the robot manipulator.

$$H_4^0 = {}_1^0T\,{}_2^1T\,{}_3^2T\,{}_4^3T \quad (3)$$

Where subscripts 1, 2, 3 and 4 are representing joints 1, 2, 3 and 4 respectively. Similarly, superscripts 0, 1, 2, 3 and 4 are representing base joint and joints 1, 2 and 3, respectively. Thus, equation 4 represents the transformation matrices from joint 1 to joint 3 are represented by the matrices from ${}^{0}_{1}T \; to \; {}^{3}_{4}T$ and the location of the 4^{th} coordinate system with respect to the base coordinate is given by H^0_4.

$$H^2_0 = {}^{0}_{1}T\,{}^{1}_{2}T \tag{4}$$

IV. Calculate the position and orientation of the end-effector.

The general homogeneous matrix for the desired position and orientation of the fingertip is shown in equation 5.

$$H^0_4 = \begin{bmatrix} r_{11} & r_{12} & r_{13} & x \\ r_{21} & r_{22} & r_{23} & y \\ r_{31} & r_{32} & r_{33} & z \end{bmatrix} = {}^{0}_{1}T\;{}^{1}_{2}T\;{}^{3}_{4}T \tag{5}$$

Considering Figure 2 (a) and (b), assuming that the total length of the hand is 165 mm. Let the lengths be l_1 = 50 mm, l_2 = 45 mm and l_3 = 35 cm. In the DH convention the only variable angle is Θ, therefore, we use c_i, s_i to denote $\cos\theta_i$, $sin\theta_i$ respectively and $\theta_1 + \theta_2$ by θ_{12} and cos $(\theta_1 + \theta_2)$ by c_{12}, sin $(\theta_1 + \theta_2)$ by s_{12} , and so on. P_x, P_y , P_z represent position vectors of the fingertip on x, y, and z axes respectively. Equations 6 - 9 were used to derive the forward kinematic equation for the robot. Hence, the forward kinematics for the robot fingertip is given in equation (10). It should be noted that equation (10) consists of two main components: the rotation matrix and the position vector of the fingertip.

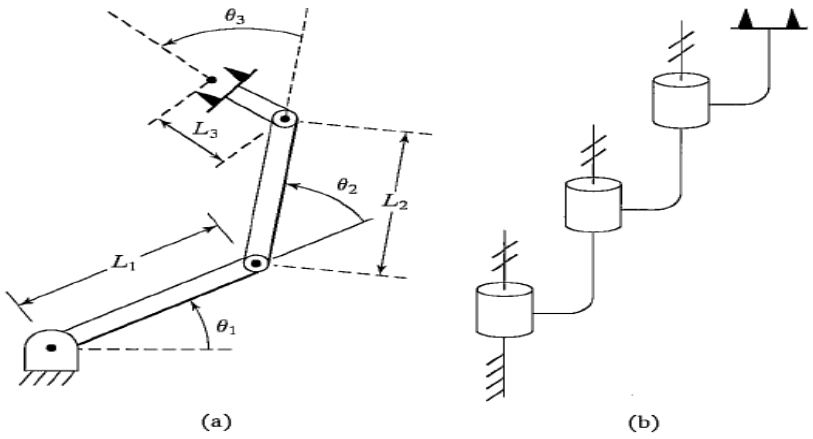

Figure 2: Three link planar model showing one finger

$$\cos(\theta_1 + \theta_2 + \theta_3) = \cos(45+90+135) = \cos 270° = 0 \tag{6}$$

$$\sin(\theta_1 + \theta_2 + \theta_3) = \sin(45+90+135) = \sin 270° = -1 \tag{7}$$

$$P_x = l_1c_1 + l_2c_{12} + l_2c_{123} = 50\cos 45° + 45\cos 135° + 45\cos 270° = 3.54 \tag{8}$$

$$P_y = l_1s_1 + L_2s_{12} + l_2s_{123} = 50\,sin45° + 45\sin 135° + 45\sin 270° = 22.14 \tag{9}$$

and $P_z = 0$

$$H^0_4 = \begin{bmatrix} 0 & 1 & 0 & 3.54 \\ -1 & 0 & 0 & 22.14 \\ 0 & 0 & 0 & 0 \\ 0 & 0 & 1 & 1 \end{bmatrix}$$ and the Fingertip position is P = [3.54 22.14 0] (10)

2.2 Inverse Kinematics

Inverse kinematics can be used as a reference angle to determine the path the tip takes to get from point A to point B. It is the solution of the angles obtained from the forward kinematics equations for the values θ_1, θ_2 and θ_3. It is possible to derive the values of the angles when [x, y] is known. Robotic manipulation tasks are challenging primarily due to inverse kinematics, which is a complex calculation of angles based on a single frame of reference. Equations 11-25 were used to determine the value angle θ_1, θ_2 and θ_3.

Considering θ_1:

From , $\theta_1 = Atan(y,x) - Atan\,(k_1,k_2)$ (11)

where link lengths, $l_1 = 50mm\,, l_2 = 45mm\,, l_3 = 35mm$

$and\ \theta_1 = 45°, \theta_2 = 90° and\ \theta_3 = 135°$

$x = k_1c_1 + k_2s_1 = (l_1c_1 + l_1c_2)c_1 - (l_2s_2)s_1 = l_1c_1 + l_2c_1c_2 - l_2s_1s_2$ (12)

$= 50 \times \cos 45° + 45 \cos 45° \cos 90° - 45 sin45° sin90° = 3.54$

$y = k_1s_1 + k_2c_1 = (l_1 + l_1c_2)s_1 + (l_2s_2)c_1 = l_1s_1 + l_2s_1c_2 + l_2c_1s_2$ (13)

$= 50 \times \sin 45° + 45 \sin 90° \cos 90° + 45 cos45° sin90° = 67.18$

Also.

$k_1 = l_1 + l_2c_2 = 50 + 45 \cos 90° = 50$ (14)

and

$k_2 = l_2s_2 = 45 \sin 90° = 45$ (15)

$\theta_1 = Atan(67.18,3.54) - Atan\,(45,50) = (86.98 - 41.98) = 45°$ (16)

Hence, $\theta_1 = 45$

Considering θ_2:

Recall that ; $\theta_2 = Atan(S_2, C_2)$ (17)

From; $s_2 = \sqrt{(1 - c_2^2)}$ (18)

$= \sqrt{(1 - cos^2\,90°)} = 1$

But

$$c_2 = \frac{x^2 + y^2 - l_1^2 - l_2^2}{2l_1l_2} \quad (19)$$

But from above; $x^2 + y^2 = l_1^2 + l_2^2 + 2l_1l_2c_2$ (20)

$x^2 + y^2 = 50^2 + 45^2 + 2(50)(45) cos90° = 4525$

By substituting into equation (19) ; we get

$$c_2 = \frac{4525 - 50^2 - 45^2}{2(50)(45)} = 0 \quad (21)$$

Hence ; $\theta_2 = Atan(1,0) = 90°$

Considering θ_3:

Recall that, $\theta_1 + \theta_2 + \theta_3 = Atan(S_\emptyset, C_\emptyset) = \emptyset \quad \leftrightarrow \quad \emptyset = (\theta_1 + \theta_2 + \theta_3)$

But ; $\theta_3 = \emptyset - (\theta_1 + \theta_2)$

$S_\emptyset = sin(\theta_1 + \theta_2 + \theta_3) = \sin 270° = -1$ (22)

$C_\emptyset = cos(\theta_1 + \theta_2 + \theta_3) = cos270° = 0$ (23)

$\emptyset = Atan(S_\emptyset, C_\emptyset) = A\tan(-1, 0) = -90°$ (24)

This implies that the $\emptyset$ is in the *third coordinate of the cartesian coordinate system*

Hence $\emptyset = (360° - 90°) = 270°$ *meaning* $\theta_3 = 270° - (45° + 90°) = 135°$ (25)

$$\therefore \quad \theta_3 = 135°$$

Hence the Final Inverse Kinematics are $\theta_1 = 45°$; $\theta_2 = 90°$; and $\theta_3 = 135°$

2.3 Dynamic Analysis

Knowledge of joint force and torque for motor selection is the main motivation for dynamics analysis. Even though the linkage is operated mechanically, it is important to understand these parameters to ensure that the correct motor that can support the weight of the linkage as well as the weight that the fingers are supporting is used. The following details, including connection length, masses, joint spacing, configuration, and connection type, must be known to calculate joint force/moment. It is also important to understand that joint force and torque are calculated using the moment principle. The parameters for the linkage analysis of the three-finger robot hand are shown in Table 2.

Weight of the lifted object (w_l) = 1 kg maximum (assumption) = 1 x 9.81 = 9.81 N and weight of the joint (w_j) = 0.005kg x 9.81 = 0.0491N. Therefore, the Cytron RC-C55S servo motor was chosen as the ideal motor for this work due to the values obtained from joint force and torque analysis of the system.

Table 2: Parameters of Three-Finger Robot Hand

Link	Mass (kg)	Weight (N)	Length (mm)	Type of Joint
Base	0. 065	0.06377	65	Revolute
1	0.013	0.1280	50	Revolute
2	0.011	0.1080	45	Revolute
3	0.010	0.0981	35	Revolute

2.4 Calculation of the Jacobian Matrix

A robot manipulator's Jacobian matrix, J_v maps the linear or first order differential relationship between its joints and Cartesian spaces. The Jacobian matrix fully describes the relationship between the end-effect velocity and the joint velocity. Each column in the J_v represents the effect on end-effector velocities due to variation in each joint velocity. Equation 26 represents the Jacobian matrix of the system.

$$J_v = \begin{bmatrix} -32.18 & 3.18 & 35 \\ 3.18 & -31.82 & 0 \\ 1 & 1 & 1 \end{bmatrix} \quad (26)$$

2.5 Control System

The entire control system for the multi-finger robot hand is described here. It shows the derivation of the mathematical model of the system, each individual component in the physical system is considered, which is added together to obtain the overall transfer function, and the analysis of design and testing is carried out using MATLAB® 7.9.0 (r2009b).

2.6 The Hand Actuator Model

The control of the robot finger is an integral part of the joint control device. These joint controls receive the desired joint deflections and output control signals in digital form, which are interpreted by the actuators after processing by a D/A converter. Each joint has a separate joint control, actuator, and speed reduction gear. The mechanism of each robot finger shall have a spring to reduce forced torques on the actuator and prevent the fingers from freely falling into positions that could prevent retrieval of the actuator; and help in responding to the control by the proportional-integral-derivative (PID) controller. Figures 3, 4 and 5 depict physical system representation, functional block diagram of the DC motor and the block diagram of the transformation of the physical system, respectively.

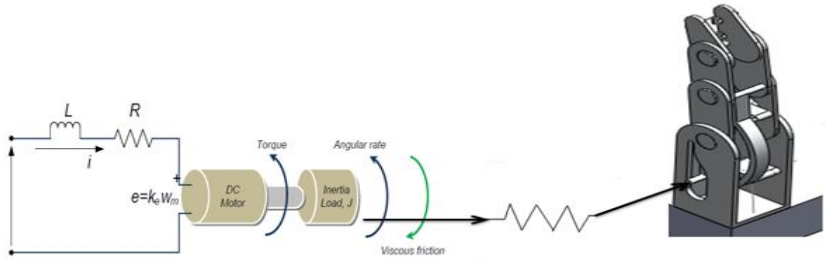

Figure 3: The Physical System of Multi-Finger Robotic Hand

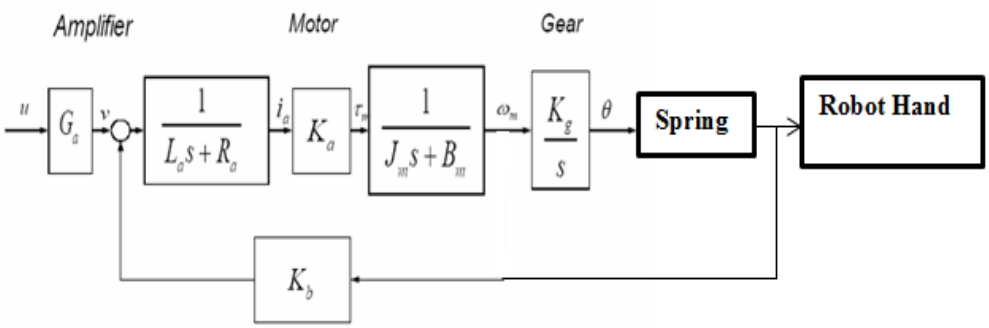

Figure 4: Schematic of Functional Block Diagram DC motor driving the Robot Hand

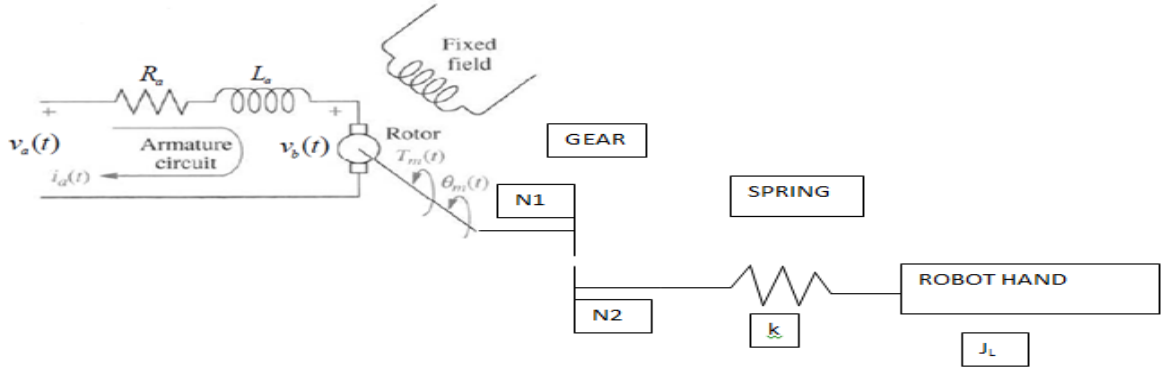

Figure 5: Functional Block Diagram representing transformation of physical system

3. RESULTS AND DISCUSSION

The kinematic analysis of the three-finger robotic hand was completed by calculating both forward and inverse kinematic equations using the Denavit-Hartenberg convention. Rotation matrices, homogeneous transformation matrices and Euler angles were used to derive the parameters required to solve the inverse kinematics problems. Additionally, the Jacobian matrix and required torques for each finger were determined. Design and testing were performed using MATLAB®c7.9.0 (R2009b), with results presented in Figures 6 - 9 and summary of the results in Tables 3 - 4. Figure 6 shows the results obtained for open step response of the system. This indicates that the step response of the system is quite sluggish in open loop when the engine is idling at start-up. The closed-loop step design significantly improved system performance, resulting in a reduction in rise time to 1.74 s and settling time to 3.09 s as shown in Figure 7.

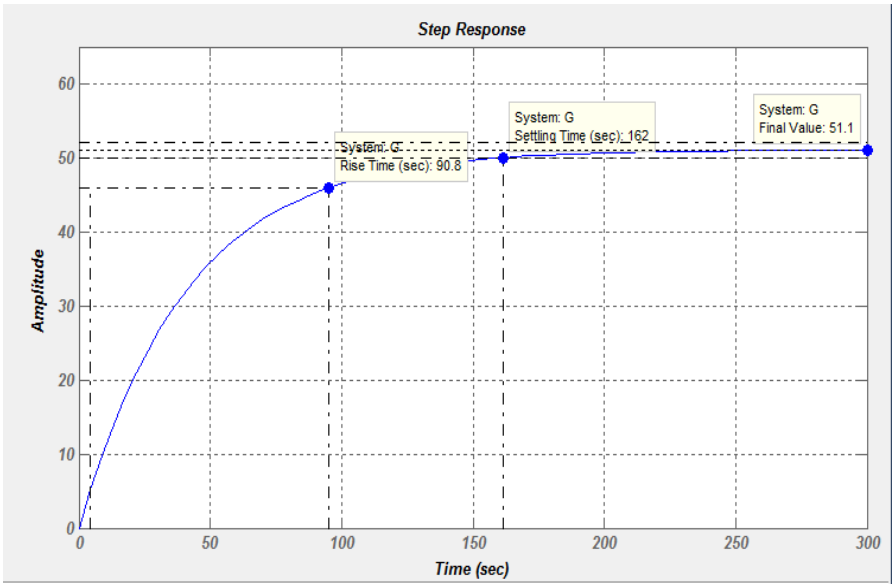

Figure 6: Open-loop step response of the System

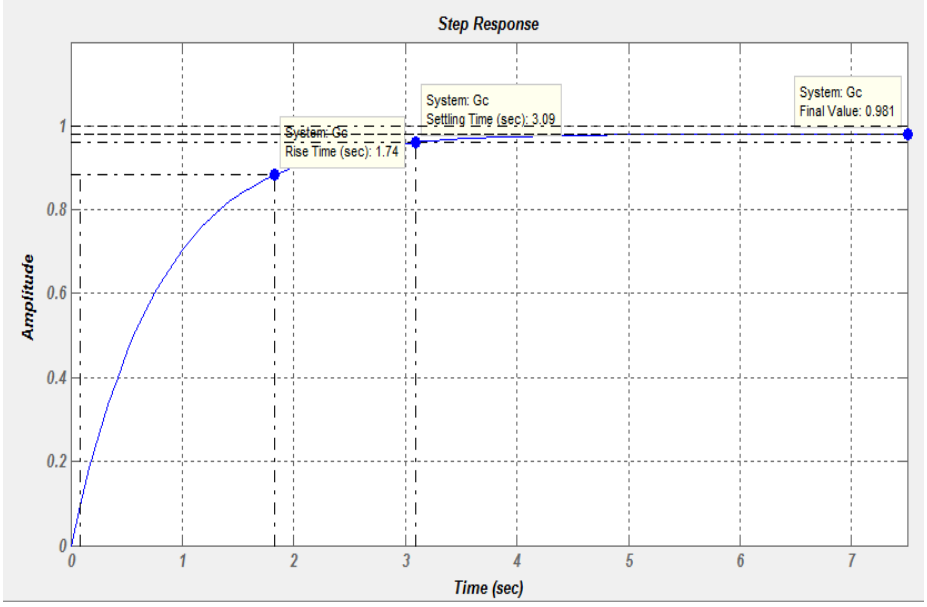

Figure 7: Closed-loop step response of the System

Table 3 shows the summary of the results obtained for both open and closed loop step response of the system. The rise time is measured at 90.8 s and the settling time at 162 s for open loop, indicating that the overall response of the system will be slow. While the rise time is measured at 1.74 s and the settling time at 3.09 s for closed loop, showing improved system performance. Figures 8 and 9 also depict the result obtained for open and closed loop ramp response of the system. Table 4 also shows the summary of the results obtained for both open and closed ramp response of the system. It measured the peak time at 0.547 s and the settling time at 162 s for open loop while the peak time is measured at 0.018 s and the settling time at 3.11 s for closed loop.

Table 3: Simulation Result of Step Response of the Robot Hand

Parameter	Open-loop	Closed-loop
Rise Time (s)	90.8	1.74
Settling Time (s)	162	3.09
Amplitude (mm)	51.1	0.981

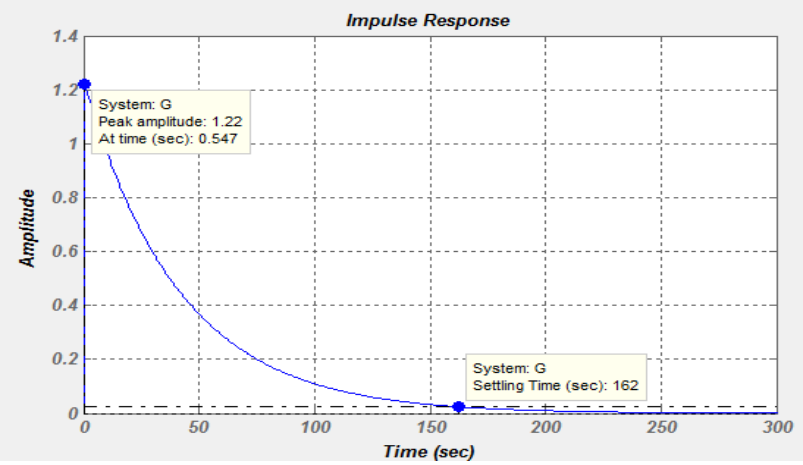

Figure 8: Open – loop Ramp response of the system

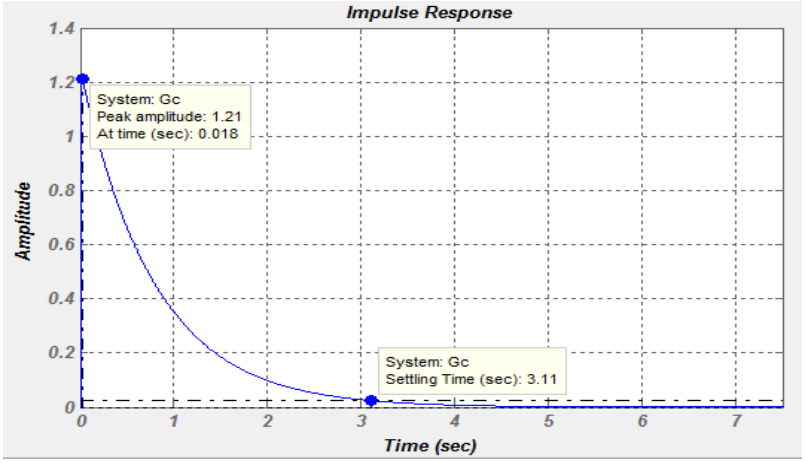

Figure 9: Closed loop Ramp response of the system

Table 4: Simulation Result of Ramp Response of the Robot Hand

Parameter	Open-loop	Closed-loop
Amplitude (mm)	1.22	0.981
Peak Time (s)	0.547	0.018
Settling Time (s)	162	3.11

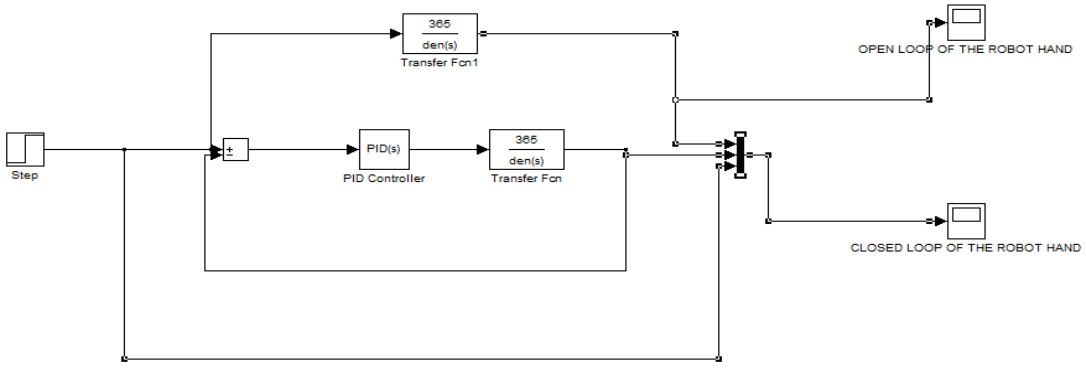

Figure 10: SIMULINK Model of the compensated Robot Hand

Figures 11-15 show the PID controller results obtained using SIMULINK and MATLAB. Figure 11 shows the open loop of the step response of the system without PID controller. Figure 12 shows curves of the step input, open-loop PID controller, and closed-loop PID controller in blue, yellow, and cyan, respectively. The closed-loop PID controller, represented by the cyan curve, shows a gradual increase followed by an overshoot from 1.5 s to 3.5 s before stabilizing. The function of this controller is to correct errors in the system by receiving feedback. Although the closed-loop PID controller cannot completely eliminate errors, it effectively reduces them. In this case, the cyan curve rises rapidly, crosses the image, decreases, and finally stabilizes after 3.5 s. The stability of the system is confirmed by the root locus plot in Figure 13, which shows that the roots of the system are in the left half of the plot. The gain value at this stable point is 0.561. Without a PID controller, Figure 14 depicts the system's open-loop step response. The straight-line nature of the curve is evident. The step response of the PID controller system is shown in Figure 15. The curve rises rapidly, with a rise time (T_r) of 0.408 s, until it reaches its peak amplitude of 1.18 at a peak time (T_p) of 1.08 s. At this point the percent overshoot (%OS) is 17.8 % and the curve then gradually decreases until it reaches a settling time (T_s) of 2.54 s and then becomes stable at an amplitude of 1.0

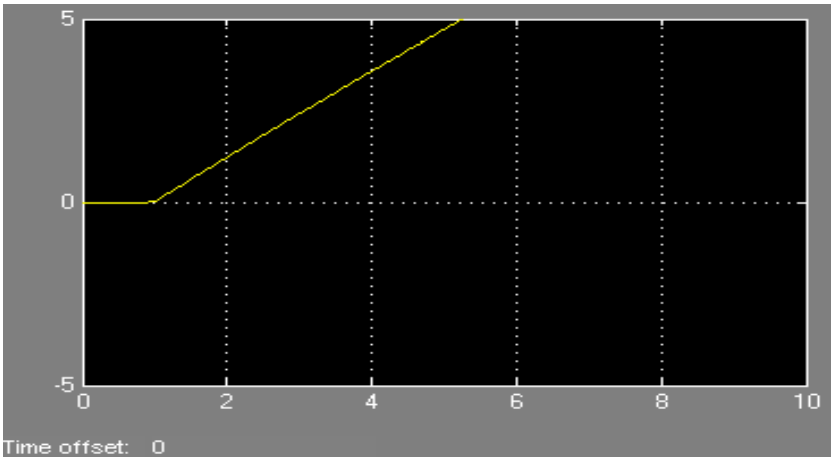

Figure 11: Open loop of the step response of the system without PID controller

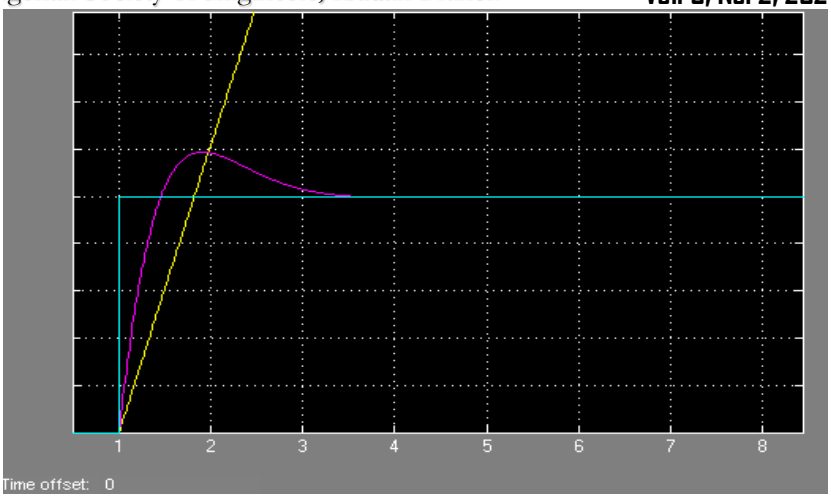

Figure 12: Closed loop of the step response of the system with PID controller

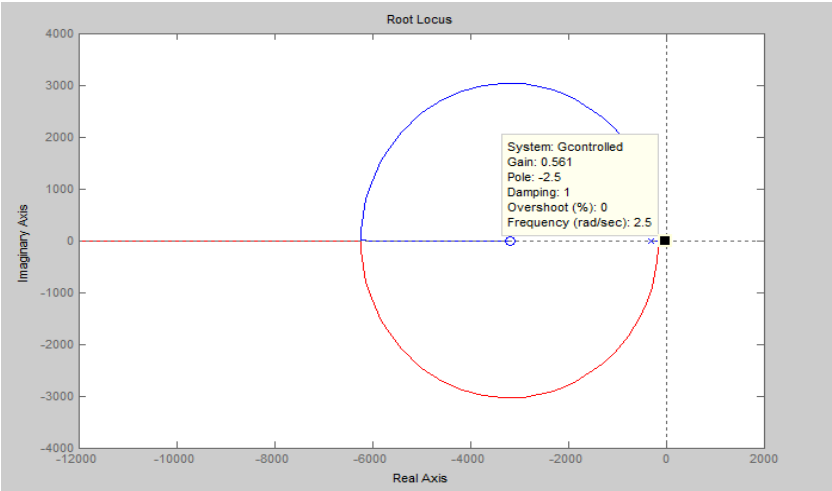

Figure 13: Root Locus Plot to verify the stability of the system

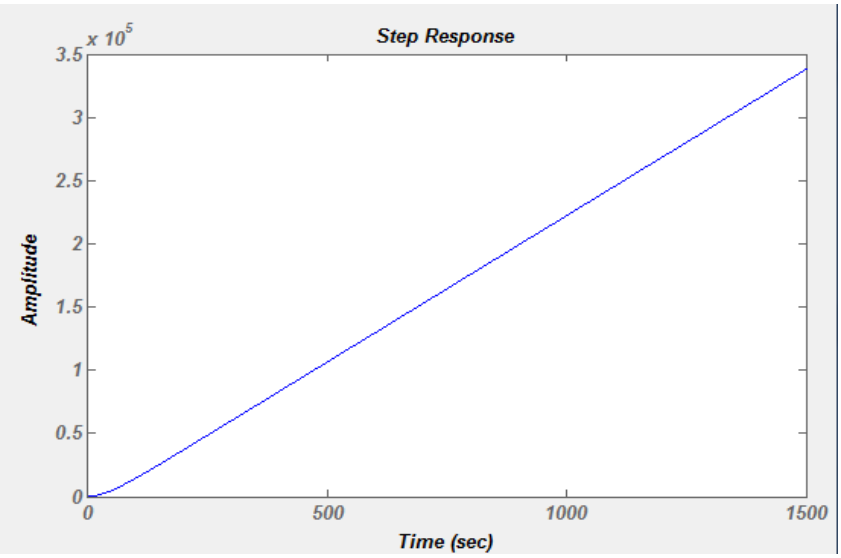

Figure 14: Open-loop step response of the system without the PID Controller

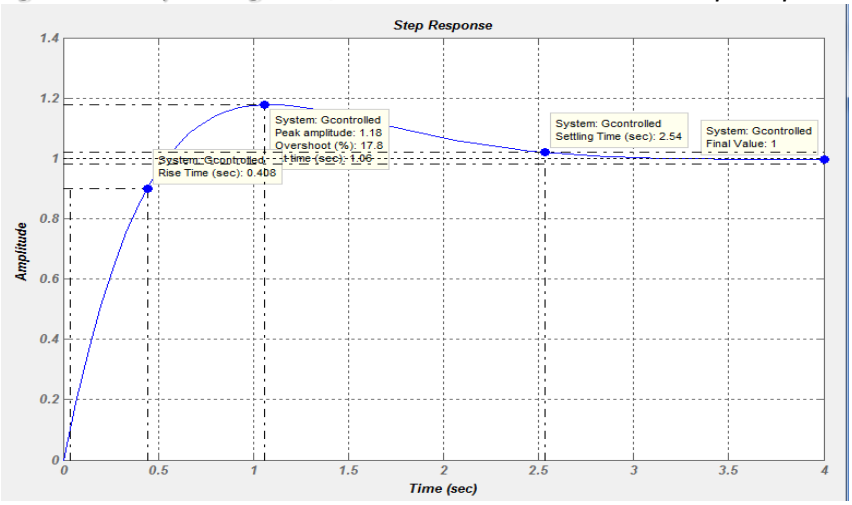

Figure 15: Closed-loop step response of the system with the PID Controller

4. CONCLUSION

The kinematic analyses of three-finger robot hand have been developed showing the forward kinematic and inverse kinematic equations by using the Denavit Hartenberg convention. These parameters are derived based on rotation matrices, homogenous transformation matrices and the usage of Euler angles to solve for angular parameters in the inverse kinematics problems. The Jacobian matrix and the torques that is required to drive each finger have also been obtained. The mathematical modelling of the motor system have been derived as well as the derivation of the transfer function of the system, showing the system block diagram, description of each block, and each components. At constant speed, the torque that the motor develops corresponds exactly to the torque that results from the mechanical load. It can be concluded from the simulation results obtained that the analysis is suitable for system control.

References

Aguilar-Pereyra, J. F. and Castillo-Castaneda, E. (2016). Design of a reconfigurable robotic system for flexoextension fitted to hand fingers size. *Applied Bionics and Biomechanics*, 1–10.

Folgheraite, M. R. and Gini, G. (2001). Human-like hierarchical reflex control for an artificial hand. *Proc. IEEE Humanoids*, Tokyo, Japan.

Hu, Z., Zhou, C., Li, J. and Hu, Q. (2023). Design of a compact anthropomorphic robotic hand with hybrid linkage and direct actuation. *International Conference on Intelligent Robotics and Applications*, vol 14270. Springer, Singapore. https://doi.org/10.1007/978-981-99-6492-5_28

Kim, U., Jung, D. and Jeong, H. (2021). Integrated linkage-driven dexterous anthropomorphic robotic hand. *Nat. Commun.*, 12(1), 7177.

Krausz, N. E. and Rorrer, R. A. (2015). Design and fabrication of a six degree-of-freedom open source hand. *IEEE Trans. Neural Syst. Rehabil. Eng.* 24(5), 562–572.

Janghorban, A., Dehghani, R (2022). Design and Motion Analysis of a Bio-Inspired Soft Robotic Finger Based on Multi-Sectional Soft Reinforced Actuator. *J Intell Robot Syst* 104, 74. https://doi.org/10.1007/s10846-022-01579-3

Liu, H. H. and Zhang, H. H. (2024). Kinematic and configuration analysis of a five-fingered metamorphic robot hand. *6th International Conference on Reconfiguration Mechanism and Robots (ReMAR).* DOI: 10.119/ReMAR61031.2024.10617699.

Massa, B., Roccella, S., Carrozza, M. C. and Dario, P. (2002). Design and development of an under actuated prosthetic hand, in: Proceedings of the 2002 *IEEE International Conference on Robotics & Automation (ICRA 2002), Washington*, pp. 3374–3379.

Mina T., Kouta, Z. and Akira, S. (2008). The co-operative control system of Robot Finger using Shaping Memory Alloys and Electrical Motors. *IEEE International Workshop on Advance Motion Control.*

Neha, E., Mukherjee, S. and Suhaib, M. (2021). An effort for determining the actuating forces in a multi-finger tendon-driven robotic hand for grasping different objects. *J Braz. Soc. Mech. Sci. Eng.* 43, 181. (https://doi.org/10.1007/s40430-021-02901-0

Psarasuraman, S. (2008). Kinematic and control system design of manipulators for a humanoid robot. *Proceedings of World Academy of Science, Engineering and Technology,* Vol ISSN 1307-6884 Pwaset Vol.

Woi, B., Shu, S. H., Zhang, Y., Yang, R., and Xing, B. (2020). Kinematic analysis and trajectory planning simulation of manipulator based on AUB-15. *4th Annual International Conference on Data Science and Business Analysis* (ICDSBA). DOI:10.1109/ICDSBA51020.2020.0025.

Yunus, Z. A. and Hacioglu, Y. (2009). Modelling and control of a humanoid robot hand finger, Faculty of Engineering, Department of Mechanical Engineering, Istanbul University, Turkey.